

Plant nuclear shape is independently determined by the SUN-WIP-WIT2-myosin XI-i complex and CRWN1

Xiao Zhou, Norman Reid Groves, and Iris Meier

Department of Molecular Genetics; The Ohio State University; Columbus, OH USA

Keywords: *Arabidopsis*, CRWN1, KASH, LINC, nuclear shape, nuclear envelope, SUN

Abbreviations: CDS, coding sequence; CRWN1, CROWDED NUCLEI 1; KASH, Klarsicht/ANC-1/Syne-1 Homology; LINC, linker of the nucleoskeleton to the cytoskeleton; NE, nuclear envelope; NLI, nuclear envelope localization index; SUN, Sad1/UNC-84; *sun1-KO sun2-KD*, *sun1-knockout sun2-knockdown*; WIP, WPP domain-interacting protein; WIT, WPP domain-interacting tail-anchored protein; XI-iC642, myosin XI-i C-terminal 642 amino acids.

Nuclei undergo dynamic shape changes during plant development, but the mechanism is unclear. In *Arabidopsis*, Sad1/UNC-84 (SUN) proteins, WPP domain-interacting proteins (WIPs), WPP domain-interacting tail-anchored proteins (WITs), myosin XI-i, and CROWDED NUCLEI 1 (CRWN1) have been shown to be essential for nuclear elongation in various epidermal cell types. It has been proposed that WITs serve as adaptors linking myosin XI-i to the SUN-WIP complex at the nuclear envelope (NE). Recently, an interaction between *Arabidopsis* SUN1 and SUN2 proteins and CRWN1, a plant analog of lamins, has been reported. Therefore, the CRWN1-SUN-WIP-WIT-myosin XI-i interaction may form a linker of the nucleoskeleton to the cytoskeleton complex. In this study, we investigate this proposed mechanism in detail for nuclei of *Arabidopsis* root hairs and trichomes. We show that WIT2, but not WIT1, plays an essential role in nuclear shape determination by recruiting myosin XI-i to the SUN-WIP NE bridges. Compared with SUN2, SUN1 plays a predominant role in nuclear shape. The NE localization of SUN1, SUN2, WIP1, and a truncated WIT2 does not depend on CRWN1. While *crwn1* mutant nuclei are smooth, the nuclei of *sun* or *wit* mutants are invaginated, similar to the reported *myosin XI-i* mutant phenotype. Together, this indicates that the roles of the respective WIT and SUN paralogs have diverged in trichomes and root hairs, and that the SUN-WIP-WIT2-myosin XI-i complex and CRWN1 independently determine elongated nuclear shape. This supports a model of nuclei being shaped both by cytoplasmic forces transferred to the NE and by nucleoplasmic filaments formed under the NE.

Introduction

Nuclear morphology changes are associated with cell polarization and migration, which are critical for cell proliferation and tissue development in eukaryotes.^{1–4} LINC complexes are essential players in nuclear shape determination and cell migration. Formed by the outer nuclear membrane Klarsicht/ANC-1/Syne-1 Homology (KASH) proteins and the inner nuclear membrane Sad1/UNC-84 (SUN) proteins at the nuclear envelope (NE), LINC complexes connect lamins, the chief component of the nucleoskeleton, to the cytoskeleton. Mutations in these proteins lead to nuclear shape abnormalities and human diseases.^{5–7}

Nuclear shape undergoes changes during plant development,^{8,9} but the mechanism is not fully understood. In *Arabidopsis* root hairs, the nuclei can reach ~40 µm in length, which is more dramatic than in other cell types.¹⁰ Elongated nuclei have also been observed in *Arabidopsis* leaf epidermal cells and trichomes.^{10,11} Recently, constituent proteins of the LINC

complexes have been reported to be essential for the elongated nuclear shape in *Arabidopsis*.^{10–12} *Arabidopsis* WPP domain-interacting protein 1 (WIP1), WIP2, and WIP3 are plant-specific KASH proteins that interact with SUN1 and SUN2 at the NE.¹⁰ The *wip1-1 wip2-1 wip3-1* triple null mutant and *SUN* mutants including the *sun1-knockout sun2-knockdown* (*sun1-KO sun2-KD*) mutant harbor round nuclei in root hairs, epidermal cells, and trichomes.^{10,12} A similar phenotype has been observed in the *wit1-1 wit2-1* double null mutant and in *myosin XI-i* mutants.¹¹ *WIT1* and *WIT2* encode WPP domain-interacting tail-anchored proteins.¹³ *WIT1* is a NE protein that interacts with WIP1, WIP2, and myosin XI-i.^{11,13} It is proposed that the force from myosin XI-i is transferred to the SUN-WIP complex through WITs, which leads to nuclear elongation.¹¹

At the nucleoplasmic side, lamins are critical for nuclear shape in mammals.¹⁴ However, no lamin homologs have been found in plant proteomes.¹⁵ Instead, Nuclear Matrix Constituent Proteins (NMCP)^{16–18} and their *Arabidopsis* homologs, CROWDED

Correspondence to: Iris Meier; Email: meier.56@osu.edu

Submitted: 10/01/2014; Revised: 12/06/2014; Accepted: 12/22/2014

<http://dx.doi.org/10.1080/19491034.2014.1003512>

NUCLEI (CRWN, also known as LITTLE NUCLEI) proteins, were identified as putative analogs of mammalian lamins in plants.¹⁵ NMCP/CRWN proteins are coiled-coil proteins isolated from plant nuclear fractions and are proposed to share structural similarity to lamins.^{15,16,19} The *Arabidopsis* genome encodes 4 CRWN genes, but only CRWN1 and CRWN4 are localized to the nuclear periphery.^{19,20} CRWN1 and CRWN4 single mutants have small, round nuclei but show no developmental phenotypes.¹⁹⁻²¹ A recent study provided evidence for an interaction of CRWN1 with SUN1 and SUN2 at the NE, and therefore, CRWN1 may be part of a plant LINC complex.²²

In this study, using *Arabidopsis* root hair and trichome nuclei, we investigated the nuclear shape determined by the putative SUN-WIP-WIT-myosin XI-i complex and CRWN1. We discovered that WIT2, but not WIT1, is essential for recruiting myosin XI-i to the plant NE and for maintaining the elongated nuclear shape. The nuclei of the *wit2-1* null mutant were invaginated and round, similar to the nuclei of *sun1-KO sun2-KD* and *myosin XI-i* mutants. A truncated WIT2 protein (designated as WIT2*) was able to partially rescue the phenotype, and was shown to interact with WIP1, WIP2, WIP3, and the C-terminus of myosin XI-i. In *sun1-KO sun2-KD* and *wit2-1*, the NE localization of the C-terminus of myosin XI-i is also impaired, supporting the existence of LINC complexes comprised of SUN, WIP, WIT2 and myosin XI-i. SUN1, SUN2, WIP1, and WIT2* are still properly localized at the NE in the *crwn1-1* null mutant, and the round nuclei of *crwn1-1* are smooth without invaginations. These data suggest that plant nuclear shape is determined independently by the LINC complexes and CRWN1.

Results

WIT2, but not WIT1, mediates the elongated nuclear shape in *Arabidopsis* root hairs and trichomes

Arabidopsis root hair and trichome nuclei, unlike the nuclei of other cell types, are nearly uniformly elongated, which ensures accurate assessments of nuclear shape. Therefore, to identify the key factor that affects the elongated nuclear shape in *Arabidopsis*, we used root hair and trichome nuclei as models. As shown in Figure 1A, in contrast to the elongated nuclear shape in wild type (Columbia ecotype, unless otherwise indicated; please see Materials and Methods for details), the nuclear shape of *wit2-1* in both cell types is round and is similar to *wit1-1 wit2-1*. Because the wild-type root hair nuclei are very elongated with additional hyper-elongated, irregularly shaped "tails," the length of the root hair nuclei was used as an index.¹⁰ For trichome nuclei, which exhibit regular spindle-like or round shape, the ratio of the width and length of the maximal cross section of a nucleus was used as a circularity index.¹⁰ As shown in Figure 1B and C, the circularity indices of *wit2-1* in both cell types are significantly different from wild type ($P < 0.01$, 2-tailed t-test) and are similar to those of *wit1-1 wit2-1* ($P > 0.05$, 2-tailed t-test). The length of *wit1-1* root hair nuclei is slightly reduced compared to wild type ($0.05 > P > 0.01$, 2-tailed t-test), and the

index of *wit1-1* trichome nuclei is indistinguishable from that of wild type (Fig. 1, $P > 0.05$, 2-tailed t-test).

To confirm that the nuclear shape phenotype of *wit2-1* was caused by a mutation in the WIT2 gene, a truncated WIT2 cDNA was cloned. WIT2 was constantly truncated in *Escherichia coli* during cloning (at least 3 independent cloning trials), resulting in a sequence encoding the WIT2 protein model At1G68910.3 (total protein length: 582aa) with the G62-L188 fragment deleted. WIT2 is a long coiled-coil protein in which the G62-L188 encodes a small part of the coiled-coil domain at the N-terminus. The resulting gene was designated as WIT2*. GFP-WIT2* driven by the WIT2 promoter (WIT2pro::GFP-WIT2*) was transformed to *wit2-1* and *wit1-1 wit2-1*. Three *wit2-1* transgenic lines and one *wit1-1 wit2-1* transgenic line were analyzed. As shown in Figure 1A-C, GFP-WIT2* was located at the NE and was able to partially complement the nuclear shape phenotype (compared to *wit2-1* and *wit1-1 wit2-1*, $P < 0.01$, 2-tailed t-test). We then performed similar complementation experiments using *wit1-1 wit2-1* transformed with GFP-WIT1 driven by the WIT1 promoter (WIT1pro::GFP-WIT1). Two independent transgenic lines, lines 1 and 3 were examined. As shown in Figure S1 A and B, WIT1pro::GFP-WIT1 failed to rescue the nuclear shape phenotype of *wit1-1 wit2-1*. However, a previously reported pollen vegetative nuclear migration phenotype was rescued in these lines, showing that WIT1pro::GFP-WIT1 is functional.²³ These data suggest that WIT2, but not WIT1, is critical for the elongated nuclear shape in *Arabidopsis* root hairs and trichomes.

SUN1 plays a predominant role in maintenance of elongated root hair and trichome nuclear shape

Since SUN and WIP are necessary for WIT NE localization and maintaining elongated nuclear shape in root hairs and trichomes,^{10,12} we examined whether each WIP and SUN gene contributes equally to the nuclear shape phenotype observed in *wit* mutants. As shown in Figure S2, *wip1-1 wip2-1*, *wip2-1 wip3-1*, and *wip1-1 wip3-1* double null mutants exhibited a similar increase in circularity index in trichome nuclei, suggesting that each WIP gene contributes equally to nuclear elongation. Trichome nuclei in the *sun1-1*, *sun1-KO*, and *sun1-KO sun2-KD* mutant lines have a similar circularity index and are statistically significantly different from wild type (Fig. 2, $P < 0.01$, 2-tailed t-test). Similarly, in root hairs, both *sun1-1* and *sun1-KO* display less elongated root hair nuclei than wild type ($P < 0.01$, 2-tailed t-test), though not as severe as *sun1-KO sun2-KD* (Fig. 2). *sun2-1* is in the Wassilewskija (Ws-4) background, which also has elongated root and trichome nuclei, and the *sun2-1* mutation does not reduce the elongated nuclear shape in both cell types (Fig. 2). These data suggest that SUN1 plays a predominant role in nuclear shape determination.

WIT2 bridges myosin XI-i to WIPs

Since WIT1 interacts with WIP1 and WIP2, the ability of WIT2* to bind WIPs was examined. GFP-WIT2* was transiently co-expressed with Myc-WIP1, Myc-WIP2, and Myc-WIP3, respectively, in *Nicotiana benthamiana* leaves. GFP-NLS-

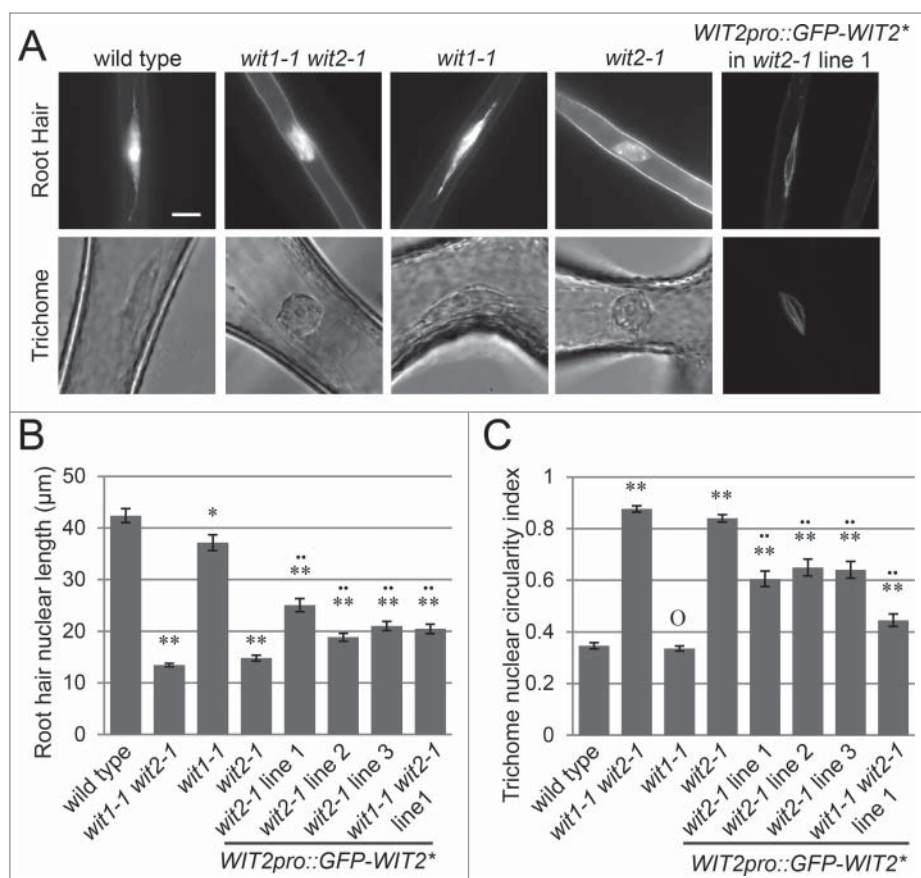


Figure 1. WIT2 is essential for the elongated nuclear shape in root hairs and trichomes. **(A)** Root hair and trichome nuclear morphology of wild type, *wit1-1 wit2-1*, *wit1-1*, *wit2-1*, and *WIT2pro::GFP-WIT2**-transformed *wit2-1*. Nuclei of *WIT2pro::GFP-WIT2**-transformed *wit2-1* were viewed using confocal microscopy. For all others, fluorescence microscopy was used to image Hoechst 33342-stained nuclei, and the trichome nuclei were imaged directly using bright field microscopy. Scale bar equals 10 μm. Images are at the same magnification scale. **(B)** Root hair nuclear shape quantified by the length of the nuclei. Single asterisk, $0.05 > P > 0.01$ when compared to wild type. Double asterisks, $P < 0.01$ when compared to wild type. Double dots, $P < 0.01$ when compared to *wit1-1 wit2-1*. Two-tailed t-test was used and $n = 80$. Error bars represent SE. **(C)** Nuclear circularity index of trichome nuclei. The ratio of width and length of the maximum nuclear cross section was used as the index. Double asterisks, $P < 0.01$, and "O," $P > 0.05$, when compared to wild type. Two-tailed t-test was used and $n = 50$. Double dots, $P < 0.01$ when compared to *wit1-1 wit2-1*. Error bars represent SE.

GFP-NES was co-expressed with Myc-WIP3 to serve as a GFP-fusion protein control. As shown in **Fig. 3A**, GFP-WIT2* co-immunoprecipitated Myc-tagged WIP1, 2 and 3, while GFP-NLS-GFP-NES did not co-immunoprecipitate Myc-WIP3.

Myosin XI-i is involved in maintaining elongated nuclear shape in *Arabidopsis*.¹¹ Its C-terminal 642 amino acid region (XI-iC642, containing the coiled coil domain and the dilute domain, but lacking the motor domain) interacts with WIT1 and is localized at the plant NE.^{11,24} Therefore, we examined the interaction between myosin XI-iC642 and WIT2*. GFP-XI-iC642 was co-expressed with Myc-WIT1 and with Myc-WIT2* in *N. benthamiana* leaves. GFP-NLS-GFP-NES was also co-expressed with Myc-WIT2* to serve as a negative control. As previously reported, Myc-WIT1 was co-immunoprecipitated by GFP-XI-iC642 (**Fig. 3B**). More importantly, Myc-WIT2* was co-immunoprecipitated by GFP-XI-iC642 but not by GFP-

NLS-GFP-NES (**Fig. 3B**). These data suggest that WIT2* is able to link myosin XI-i to the SUN-WIP LINC complex.

To further investigate whether WIT2 and SUN proteins are necessary for recruiting myosin XI-i to the NE, GFP-XI-iC642 was expressed under the cauliflower mosaic virus 35S promoter in wild type, *sun1-KO sun2-KD*, *wit1-1*, and *wit2-1*, respectively. As shown in **Figure 3C**, GFP-XI-iC642 was properly localized at the NE in wild type and *wit1-1* root hairs, but a decrease in NE enrichment was observed in *sun1-KO sun2-KD* and *wit2-1*. NE enrichment was quantified using the nuclear localization index (NLI).¹⁰ In short, a line was drawn across a cell and through the NE, and the ratio of the sum of the two maximum NE intensities and the sum of the two maximum cytoplasmic intensities was calculated. The NLI of GFP-XI-iC642 in *wit2-1* and *sun1-KO sun2-KD* (**Fig. 3D**) is significantly decreased when compared to wild type ($P < 0.01$, 2-tailed t-test). The NLI of *sun1-KO sun2-KD* is slightly larger than *wit2-1*, which can be explained by the residual SUN2 protein in this mutant. In contrast, *wit1-1*, which has relatively normal nuclear shape, has a NLI similar to wild type ($P > 0.05$, 2-tailed t-test). These data suggest that WIT2 bridges myosin XI-i to the SUN-WIP complex and that a LINC complex is formed that involves SUN, WIP, WIT2, and myosin XI-i.

The NE localization of SUN1, SUN2, WIP1, and WIT2* does not depend on CRWN1

Mutations in *CRWN1* or *CRWN4* lead to small, round nuclei, and *CRWN1* plays a more predominant role in this phenotype than *CRWN4*.²¹ In addition, a recent study provided evidence suggesting the interaction between CRWN1 and SUN proteins at the NE.²² Therefore, CRWN1 may be essential for the NE localization of the SUN-WIP-WIT2-myosin XI-i complex. To address this question, the NE localization of SUN1, SUN2, WIP1, and WIT2* was examined in root hairs of *crwn1-1*. The NE localization of these proteins was quantified using the NLI illustrated in **Figure 3D**. As shown in **Figure 4**, SUN1 and SUN2 were properly localized at the NE in *crwn1-1* when compared with wild type ($P > 0.05$). The NE localization of WIP1 was slightly decreased ($p = 0.035$), but the NE localization of WIT2* was not affected ($P > 0.05$). Since CRWN1 is co-localized with DNA during mitosis,¹⁹ and plays a role in

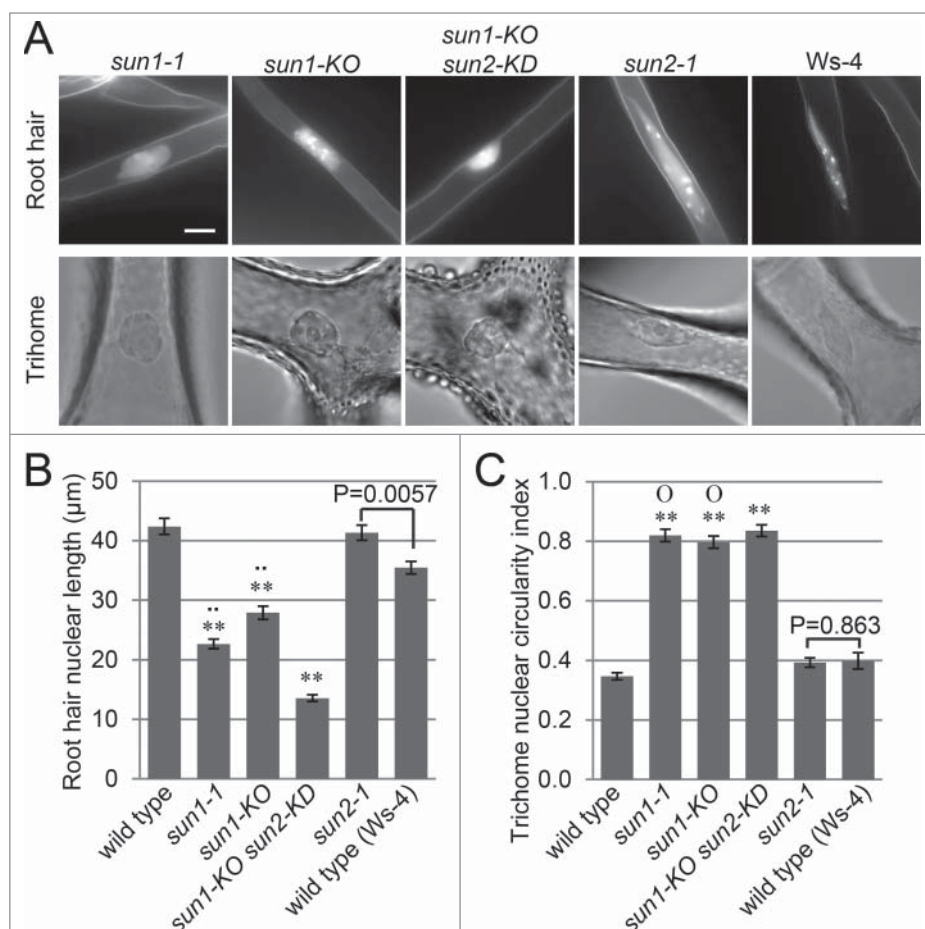


Figure 2. SUN1 plays a predominant role in nuclear shape determination. (A) Root hair and trichome nuclear morphology of *sun1-1*, *sun1-KO*, *sun2-1*, and *sun1-KO sun2-KD*. Fluorescence microscopy was used to image Hoechst 33342-stained nuclei, and the trichome nuclei were imaged using bright field microscopy. Scale bar equals 10 μm. Images are at the same magnification scale. (B) Root hair nuclear shape quantified by the length of the nuclei. Double asterisks, $P < 0.01$, when compared to wild type. Double dots, $P < 0.01$ when compared to *sun1-KO sun2-KD*. The P value of the t-test between *sun2-1* and Ws-4 is indicated in the figure. Two-tailed t-test was used and $n = 80$. Error bars represent SE. (C) Nuclear circularity index of trichome nuclei. The ratio of width and length of the maximum nucleus cross section was used as the index. Double asterisks, $P < 0.01$, when compared to wild type. "O," $P > 0.05$ when compared to *sun1-KO sun2-KD*. The P value of the t-test between *sun2-1* and Ws-4 is indicated in the figure. Two-tailed t-test was used and $n = 50$. Error bars represent SE.

chromatin organization during interphase,²¹ we examined the expression level of *SUN1*, *SUN2*, *WIP1*, and *WIT2* in *crwn1-1*. As shown in Fig. S3, no significant difference in the expression level was observed when compared with wild type. These data suggest that loss of *CRWN1* does not impact the SUN-WIP-WIT2 complex at the NE. We further noticed that the NE morphology of *crwn1-1* is smooth, which is different from the invaginated nuclei of *sun1-KO sun2-KD* and *wit2-1* (Fig. 5A). This observation was confirmed by quantification (Fig. 5B). It has been reported that the NE of *myosin XI-i* mutants is also invaginated,¹¹ supporting the hypothesis that myosin XI-i acts in the same pathway as SUN proteins and WIT2.

In summary, our data suggest a model of nuclear shape determined independently by the SUN-WIP-WIT2-myosin XI-i

complex and CRWN1 (Fig. 6). We propose that the SUN-WIP-WIT2-myosin XI-i complex transfers the cytoplasmic motor forces to the NE, while CRWN1 regulates nuclear shape by forming lamina-like structures at the nucleoplasmic side.

Discussion

Functional divergence of protein homologs

WIT1 and WIT2 have a high percentage of amino acid sequence identity (34%) and similarity (56%), and similar expression patterns.¹³ A recent study has shown that both WIT1 and WIT2 are involved in male fertility.²³ Here, we reported that only WIT2 is required for the elongated nuclear shape in root hairs and trichomes (Fig. 1 and Fig. S1). Similarly, SUN1 and SUN2 are closely related (their protein sequences are 62% identical and 72% similar),²⁵ but SUN1 is predominant in nuclear shape determination. This functional divergence among protein homologs is also found in the newly identified KASH proteins SINE1 and SINE2. SINE1 is associated with F-actin and plays a role in guard cell central nuclear anchorage, while SINE2 contributes to innate immunity against an oomycete pathogen.²⁶ This suggests that closely related paralogs of plant nuclear envelope-associated proteins have adapted to specific functions, which should be considered when addressing their biological roles.

Model for nuclear shape determination

In this study, we provide evidence that myosin XI-i is anchored to the SUN-WIP complex at the NE through WIT2. As has been proposed, the myosin XI-i motor force can thus be transferred to the NE and cause an elongated nuclear shape.¹¹ Disrupting the SUN-WIP-WIT2-myosin XI-i complex leads to invaginated, round nuclei, which is different from the smooth, round nuclei of *crwn1-1*. Our data also show that loss of CRWN1 does not affect localization of the SUN-WIP-WIT2 complex, suggesting that CRWN1 acts independently. Other NE proteins that play a role in nuclear shape include KAKU4, CRWN4, and NUP136. KAKU4 is a newly identified inner nuclear membrane-associated protein that interacts with CRWN1.²⁷ *KAKU4* mutants have spherical epidermal nuclei.²⁷ Overexpressing KAKU4 caused nuclear membrane deformation,

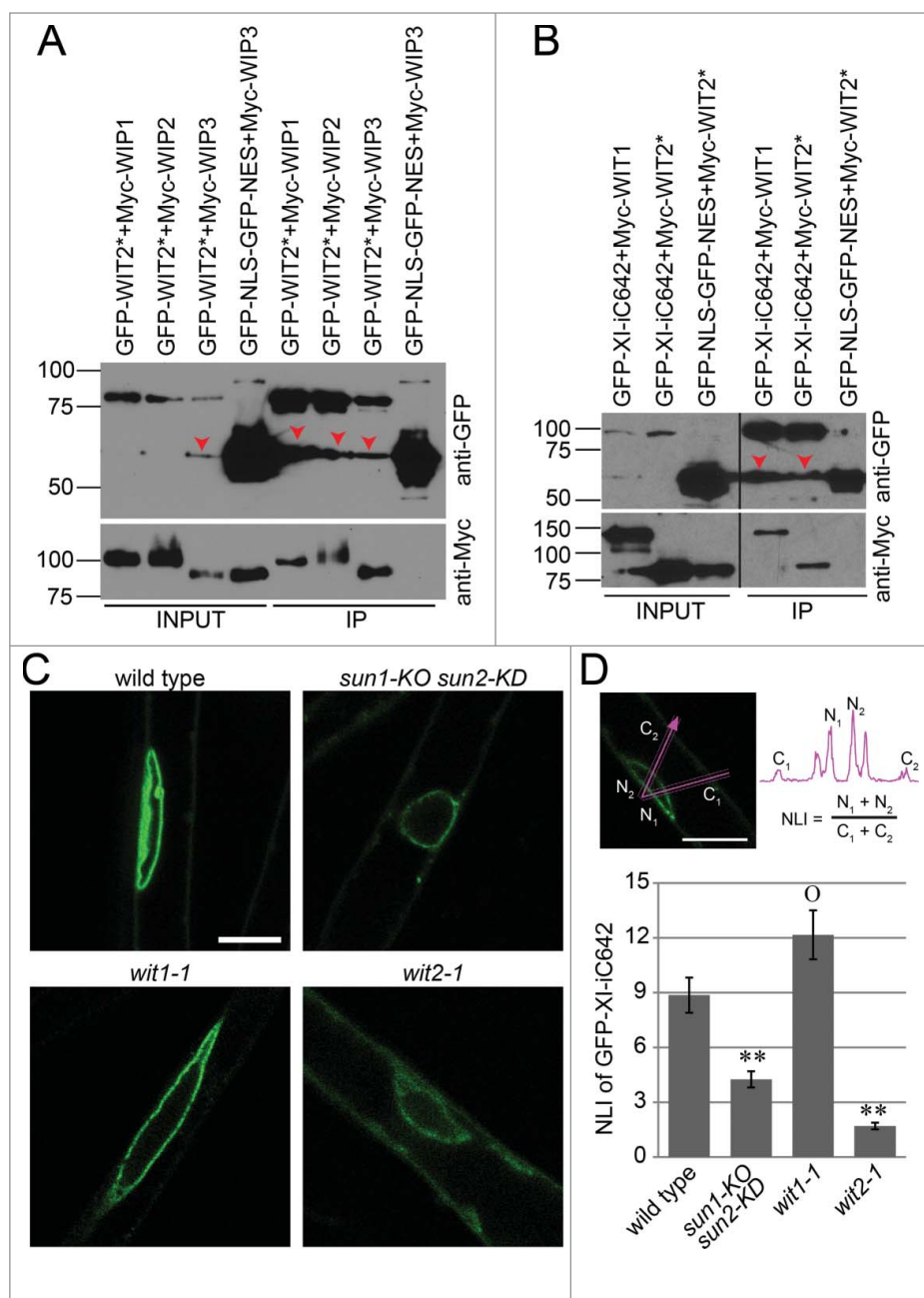


Figure 3. WIT2 connects myosin XI-i to the SUN-WIP NE bridges. **(A)** WIT2* interacts with WIP1, WIP2, and WIP3. GFP-tagged proteins were immunoprecipitated and detected with anti-GFP antibody. Myc-tagged proteins were detected with an anti-Myc antibody. Input/IP ratio was 1:9. Numbers on the left indicate molecular mass in kilodaltons. Red arrow heads indicate possible truncated GFP-fusion proteins. **(B)** WIT1 and WIT2* interacts with XI-iC642. GFP-tagged proteins were immunoprecipitated and detected with anti-GFP antibody. Myc-tagged proteins were detected with an anti-Myc antibody. Input/IP ratio was 1:18. Numbers on the left indicate molecular mass in kilodaltons. Red arrow heads indicate possible truncated GFP-fusion proteins. Vertical back lines represent intervening lanes removed for display purposes. **(C)** Localization of GFP-XI-iC642 in wild type, *sun1-KO sun2-KD*, *wit1-1*, and *wit2-1*. Scale bar equals 10 μ m. All images are single optical sections at the same magnification. **(D)** NLI of GFP-XI-iC642 in wild type, *sun1-KO sun2-KD*, *wit1-1*, and *wit2-1*. The sum of the 2 maximum NE intensities divided by the sum of the 2 maximum cytoplasmic intensities was used as an NLI (illustrated in the top panel). Double asterisks, $P < 0.01$, and "O," $P > 0.05$, when compared to wild type. Two-tailed t-test was used. For each genotype, 3 transgenic lines and 10 nuclei from each line were analyzed (total $n = 30$). Error bars represent SE.

and co-overexpressing KAKU4 with CRWN1 enhanced this deformation.²⁷ Therefore, KAKU4 has been proposed to be a putative component of plant lamina-like structures.²⁷ CRWN4 is a homolog of CRWN1 that is also localized at the NE.¹⁹ CRWN4 mutants have similar nuclear shape change to CRWN1 mutants, except that CRWN4 mutants still have tail-like projections on their spherical nuclei.¹⁹⁻²¹ Overexpressing CRWN4 in leaf epidermal cells caused abnormally elongated nuclei,¹⁹ a phenotype that is similar to NUP136-overexpressing plants.²⁸ Nucleoporin NUP136 is considered a functional homolog of animal NUP153, and its mutants also have spherical nuclei.²⁸ Since NUP153 physically interacts with lamins at the nucleoplasmic side, it has been proposed that plant NUP136 also interacts with plant lamin-like proteins.^{15,27,29} These pieces of evidence indicate that the plant nuclear shape is orchestrated by the cytoplasmic motor forces transferred through the LINC complexes and by nucleoplasmic lamina-like structures formed by CRWN1, CRWN4, KAKU4, and NUP136.

The relationship between CRWN1 and LINC complexes

In mammalian cells, the NE localization of SUN2 and the KASH protein, Nesprin-2, depends on lamin A/C.³⁰⁻³² In *Drosophila*, the NE localization of the SUN protein Klaroid, and the KASH protein Klarsicht, depends on the lamin encoded by *Dm0*.^{33,34} In *Arabidopsis*, our data show that the NE localization of SUN1, SUN2, or WIT2* does not depend on CRWN1, and the NE localization of WIP1 is only slightly affected by the loss of CRWN1 (Fig. 4). It is possible that CRWN4 might serve as a redundant NE anchor of SUN proteins. It is also possible that the NE localization of CRWN1 depends on SUN proteins, because a recent study has shown that 1) expressing SUN proteins affects the NE localization and the mobility of CRWN1, and 2) CRWN1 and SUN protein interact with each other as determined by fluorescence resonance energy transfer.²²

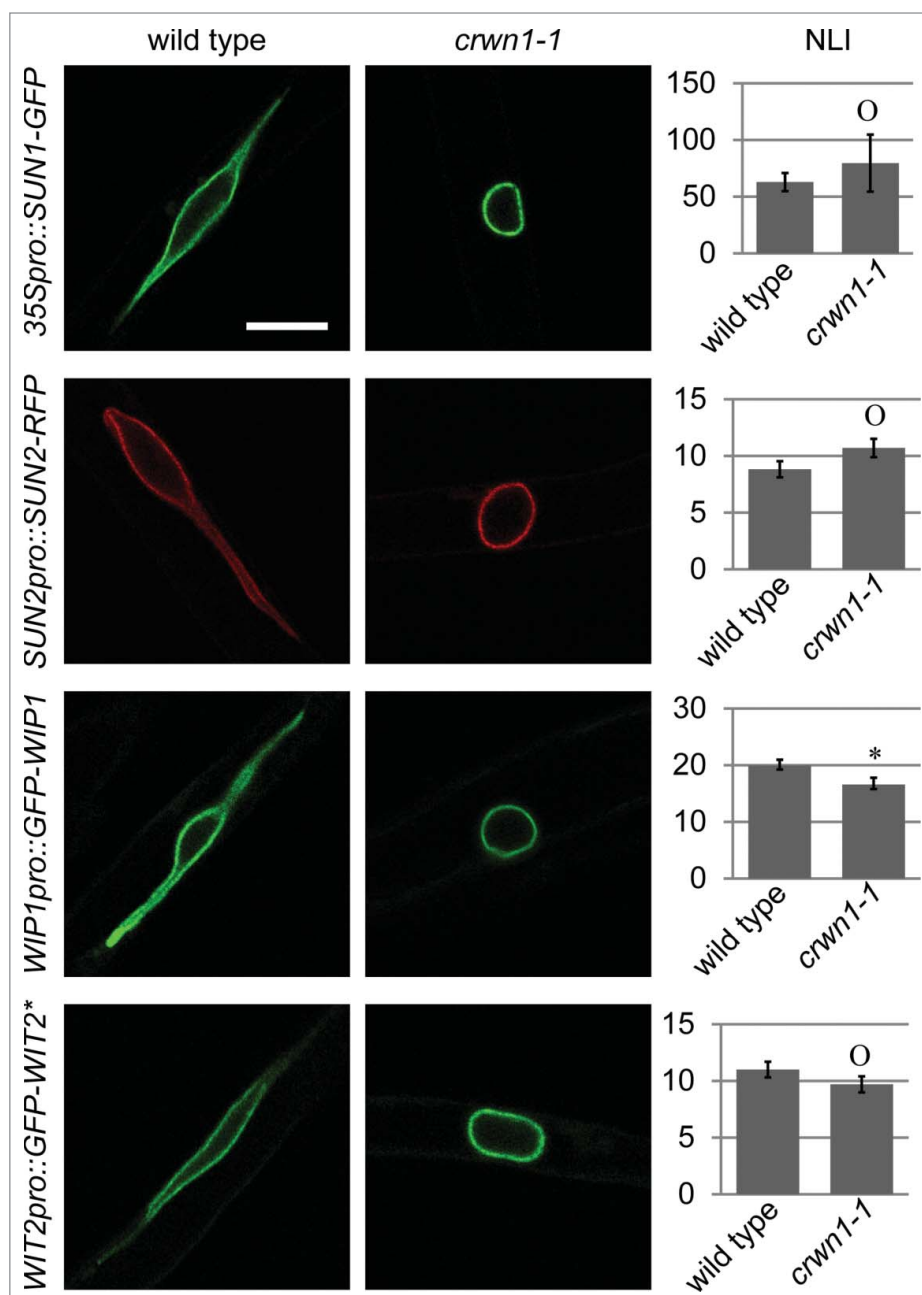


Figure 4. CRWN1 is not required for the NE-association of the SUN-WIP-WIT2 complex. The localization of SUN1-GFP, SUN2-RFP, GFP-WIP1, and GFP-WIT2* in wild type (left column) and *crwn1-1* (middle column) are shown. Scale bar equals 10 μ m, and all images are at the same magnification. The NLI are shown in the right column. Asterisk, $p = 0.035$, and "O," $P > 0.05$, when compared to wild type. For each genotype, 3 transgenic lines and 30 nuclei from each line were measured (total $n = 90$). Error bars represent SE.

Potential functions of an elongated nuclear shape

Although the epidermal nuclear shape is changed in *sun1-KO*, *sun2-KD*, *wit2-1*, *CRWN1* mutants, and *myosin XI-i* mutants, these mutations do not appear to affect plant development and physiology. One phenotype associated with the nuclear shape change is altered nuclear movement. Impaired root nuclear movement has been observed in *wit1-1 wit2-1* and *myosin XI-i*

mutants.¹¹ Dark-induced nuclear movement in leaf mesophyll cells is also impaired in *wit1-1 wit2-1* and *myosin XI-i* mutants, but light-induced nuclear movement is not disrupted.¹¹ Light-induced nuclear movement defects have not been observed in either *CRWN1* or *CRWN4* mutants.¹⁹ Lack of plant growth phenotypes under standard laboratory conditions in these mutants currently leaves the biological role of the elongated nuclear shape a puzzle. One possible function of elongated nuclear shape in root hairs and epidermal cells is to reduce physical resistance during nuclear migration. Nuclear migration has also been shown to be associated with plant-microbe interactions.^{35,36} Upon microbe invasion or symbiotic interaction, quick nuclear migration to the microbe contacting site is one of the early plant responses. Since a single root hair cell can reach a length visible to the naked eye, an elongated nuclear shape might be suitable for agile nuclear migration over a long distance. Studying genes that determine nuclear shape could thus help to uncover the function of the nucleus in plant-microbial interactions.

Materials and Methods

Plant materials

Arabidopsis thaliana were grown at 25°C in soil under 16-h light and 8-h dark or on Murashige and Skoog (Caisson laboratories, MSP01-50LT) medium with 1% sucrose under constant light. *wip1-1*, *wip2-1*, *wip3-1*, *wit1-1*, and *wit2-1* have been reported previously.^{13,37} *sun1-KO* and *sun1-KO sun2-KD* were gifts from Dr. Susan Armstrong and K. Osman (University of Birmingham, UK) and have been reported previously.¹⁰ *sun1-1* (WiscD-sLox330H03) has been reported previously¹² and was obtained from the *Arabidopsis* Biological Resource Center.

sun2-1 (FLAG_625B02) is in *Ws-4* background with a T-DNA inserted in the second exon (confirmed by sequencing) and was obtained from the Versailles *Arabidopsis* Stock Center. For genotyping *sun2-1*, the following primers were used. LP: 5'-CCGTCACGACGACCAAAACATGGGTT-3', RP: 5'-TGAGT-TAAATGCTAAAAGACGGGTTTCATAGCAAAGCGGTT-3'; and RB4: 5'-TCACGGGTTGGGGTTTCTACAGGAC-3'. As

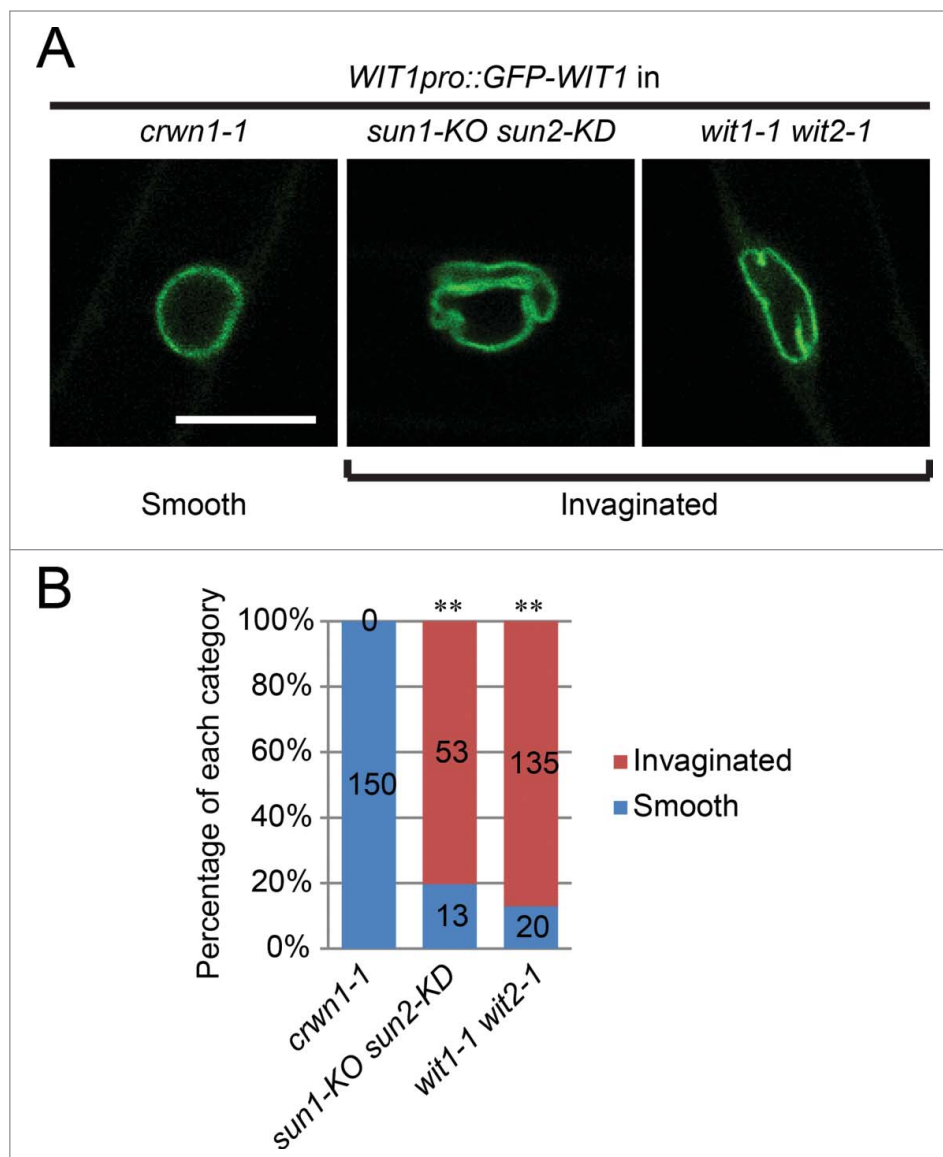


Figure 5. Root hair nuclear morphology of *crwn1-1* is different from *sun1-KO sun2-KD* and *wit1-1 wit2-1*. (A) NE morphology illustrated by GFP-WIT1. The nuclei of *crwn1-1* are smooth, while the nuclei of *sun1-KO sun2-KD* and *wit1-1 wit2-1* are predominantly invaginated. Scale bar equals 10 μ m. All images are at the same magnification. (B) Quantification of smooth nuclei and invaginated nuclei in *crwn1-1*, *sun1-KO sun2-KD*, and *wit1-1 wit2-1*. Double asterisks, $P < 0.01$, when compared with *crwn1-1*, 2-tailed Fisher's exact test. The n of each category is indicated in the figure.

shown in Fig. S3, *sun2-1* is a null mutant with no full *SUN2* length transcripts made. *crwn1-1* (SALK_025347) has been reported previously²⁰ and was obtained from the *Arabidopsis* Biological Resource Center. All *wip*, *wit*, *sun1*, and *crwn1* mutants used in this study are in Columbia background, and the Columbia ecotype was used as "wild type." For *sun2-1*, Ws-4 was used as "wild type." *N. benthamiana* plants were grown at 28°C in soil under constant light.

Constructs

The *WIT2* promoter (~2.2kb upstream the start codon of *WIT2*) was amplified by PCR from *Arabidopsis* DNA using 5'-

GGCCCGGCGCGCCACTGAT-GAATCATTACCAAGAGTGGT-3' and 5'-CTCGCCCTTGCTCAC-CATTGACTCCACAAAAAATC-TATC-3', and cloned into the *PmlI*-digested pHOAG²⁶ by In-fusion (Clontech, 639684) recombination. After confirmation by sequencing, the pHWIT2proAG vector was obtained. *WIT2* CDS was cloned from *Arabidopsis* whole seedling cDNA using 5'-GGGGACAAGTTTGTACAAAAAAGCAGGCTTTATGGAGGAAAT-CATTAGGGAGGAC-3' and 5'-GGGGACCACTTTGTACAAGAAAGCTGGGTATTAATAAGTCA-CACCAAAGAATGAA-3', and cloned into pDONR221 (Life Technologies, 12536-017) by a BP reaction (Life Technologies, 11789-020). After sequencing, we found that the T182-C562 fragment of the *WIT2* CDS was constantly (3 independent cloning trials) lost in *E. coli*, resulting in a sequence encoding the *WIT2* gene model At1G68910.3 with the protein sequence G62-L188 deleted. This truncated *WIT2* was named *WIT2**. *WIT2** CDS was then moved from pDONR221 to pHWIT2proAG by an LR reaction (Life Technologies, 11791-020) to obtain the *WIT2pro::GFP-WIT2** construct. *WIT2** CDS in pDONR221 was also cloned into pH7WGF2³⁸ and pGWB21³⁹ by an LR reaction to obtain 35S promoter-driven *GFP-WIT2** and *Myc-WIT2**, respectively. *WIP1*, *WIP2*, *WIP3*, and *WIT1* CDS cloned in pENTR/D-TOPO were reported previously,^{37,13} and were moved to pGWB21 by LR reactions to obtain 35S promoter-driven *Myc-WIP1*, *Myc-WIP2*, and *Myc-*

WIP3, respectively.

pH7RWG2³⁸ was digested with *XbaI* and *SpeI* and the fragment containing the Gateway cassette was ligated to *XbaI*-digested pPZP-Hyg-RCS2 vector²⁶ to obtain the pHAR vector. *SUN2* CDS without the stop codon was amplified by PCR using 5'-ATTCTGTAGTTCAAAATTGAAGATCATGTCGGCGT-CAACGGTGTCAATCA-3' and 5'-AGCATGAGCAACAGAGACTGAGTCTAG-3'. *SUN2* promoter (~2kb upstream of the ATG) was amplified by PCR using 5'-CACCTATC-GAGTTTGGCCGAGGAGATGCCAATTC-3' and 5'-GGTGATTGACACCGTTTACGCGGACATGATCTT-CAATTTTGAACCTACAGA-3'. The DNA fragment containing

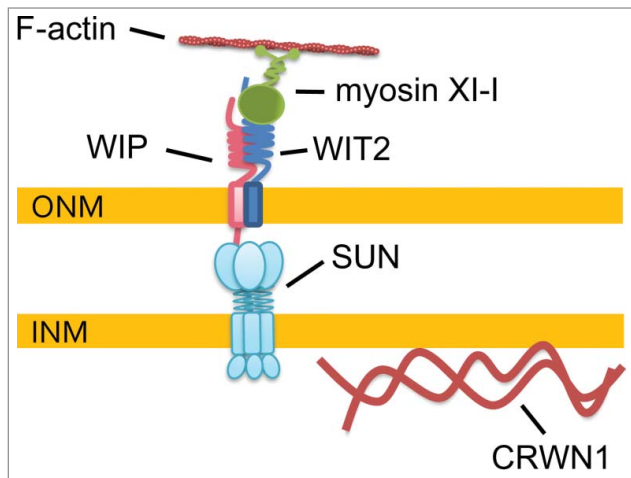


Figure 6. Model of nuclear shape determination. Myosin XI-i is anchored to the SUN-WIP NE bridges by WIT2. This SUN-WIP-WIT2-myosin XI-i complex transfers cytoplasmic forces to the NE. In the nucleoplasm, CRWN1 acts independently on nuclear shape determination by forming lamina-like structures. Other nucleoplasmic proteins that affect nuclear shape—CRWN4, KAKU4, and NUP136—and the CRWN1-SUN interaction of unknown function are not drawn.

SUN2 promoter and CDS was then amplified by overlapping PCR using the above 2 PCR products as templates and the following primers: 5'-CACCTATCGAGTTTGCCCGAGGAGATGCCAATTC-3' and 5'-AGCATGAGCAACAGAGACTGAGTCTAG-3'. The SUN2 promoter-CDS fragment was then cloned into pENTR/D-TOPO, confirmed by sequencing, and then moved to pHAR by LR reactions to obtain the *SUN2pro:SUN2-RFP* construct. SUN1 CDS was amplified by PCR using 5'-CACCATGTCGGCATCAACGGTGTGCG-3' and 5'-TTCACCTTTCAGGTGAAAGATCCTG-3'. The PCR product was cloned into pENTR/D-TOPO, confirmed by sequencing. The CDS was then moved to pB7FWG2³⁸ to obtain the *35Spro:SUN1-GFP* construct.

Agrobacterium transformation

Agrobacterium tumefaciens strain ABI was transformed with the corresponding constructs by triparental mating.⁴⁰ In brief, the *E. coli* carrying the constructs of interest were co-incubated overnight at 30°C on lysogeny broth agar (1.5%) plates with *Agrobacterium* ABI and the *E. coli* helper strain containing the vector pRK2013. Then, the bacterial mixture was streaked on lysogeny broth agar (1.5%) plates with proper antibiotics to select transformed *Agrobacterium* which was confirmed by PCR.

N. benthamiana transient transformation

Agrobacterium cultures containing plasmids expressing the proteins of interest were co-infiltrated transiently into *N. benthamiana* leaves as described previously.²⁴ In brief, *Agrobacterium* cultures were collected by centrifuging and resuspended to OD₆₀₀ = 1.0 in the infiltration buffer containing 10 mM MgCl₂, 10 mM MES, pH 5.4, and 100 μM acetosyringone (Sigma-Aldrich, D134406-1G). The *Agrobacterium* suspension

was pressure infiltrated into *N. benthamiana* leaves with a plastic syringe. Plants were grown for 2–3 d before being collected for the subsequent experiments.

Arabidopsis stable transformation

Transgenic *Arabidopsis* plants were obtained by *Agrobacterium*-mediated floral dip.⁴¹ *Agrobacterium* strains carrying the constructs of interest were inoculated in lysogeny broth liquid medium and grown overnight at 30°C. The bacteria were collected by centrifuging and resuspended in transformation solution containing 5% sucrose and 300 μL/L silwet L-77 (Lehle Seeds, VIS-01) to OD₆₀₀ = 0.8. The inflorescence of *Arabidopsis* was dipped in the bacterial suspension. After being kept moist in the dark overnight at room temperature, the plants were moved to a growth chamber and allowed to set seeds. The transgenic plants were selected on Murashige and Skoog agar (0.8%) plates containing proper antibiotics.

Co-immunoprecipitation experiments

N. benthamiana leaves were collected, ground in liquid nitrogen into powders, and Co-IP experiments were performed at 4°C. One ml NP-40 buffer (50 mM Tris-HCl, pH 7.5, 150 mM NaCl, 0.5% NP-40, 1 mM EDTA, 3 mM DTT, 1 mM PMSF, and 1% protease inhibitor cocktail [Sigma-Aldrich, P9599-5ML]) was used to extract 500 μL plant tissue. One-tenth of each protein extract was used as an input sample, and the rest was used for IP using protein A-sepharose beads (GE Healthcare) pre-coated with an anti-GFP antibody (Abcam Cambridge, ab290). After three washes using NP-40 buffer, the immunoprecipitates and the input samples were separated by 8% SDS-PAGE, transferred to PVDF membranes (Bio-Rad, 162-0177), and detected with an anti-GFP (1:2000, Clontech, 632569,) or anti-Myc (1:1000, Sigma-Aldrich, M5546) antibody.

Confocal microscopy

Six- to 8-day old *Arabidopsis* seedlings were imaged using a Nikon Eclipse C90i confocal microscope with small or medium pinhole and gain setting range of 7.0 to 7.5. The 488nm laser was set at 30–50% power for imaging *35Spro:GFP-XI-iC642* transgenic plants whose transgene expression was low in all lines, while the other transgenic lines and *N. benthamiana* leaves were imaged using 10%–30% laser power. All images were taken at room temperature using Murashige and Skoog medium as medium with Nikon Plan Apo VC 60x H lens (numerical aperture 1.4). The transmitted light detector was turned on to collect transmitted light signal simultaneously. Images were exported to PNG format by Nikon NIS-Elements software and organized in Adobe Photoshop and Illustrator. Intensity readings were performed in Nikon NIS-Elements software.

Hoechst 33342 staining

Six- to 8-d old *Arabidopsis* seedlings grown on Murashige and Skoog plates were used. Samples were stained for 20 min in a phosphate buffered saline (pH 7.4) solution containing 4 μM Hoechst 33342 (Thermo Scientific, 28491-52-3) and 4%

paraformaldehyde (Sigma-Aldrich, 76240). Root hair nuclei images were taken by a Nikon DS-Qi1Mc digital camera. The length of the nuclei was measured using the Nikon NIS-Elements software.

RT-PCR analysis

Leaves of 20-day-old *Arabidopsis* plants were ground in liquid nitrogen and total RNA was extracted using the RNeasy Plant Mini Kit (Qiagen, 74903). First strand cDNA was synthesized using the SuperScript® III First-Strand Synthesis System (Life Technologies, 18080-051) and oligo dT as primer. Primers used for PCR were listed in Table S1.

References

1. Gladfelter A, Berman J. Dancing genomes: fungal nuclear positioning. *Nat Rev Microbiol* 2009; 7:875-86; PMID:19898490; <http://dx.doi.org/10.1038/nrmicro2249>
2. Starr DA, Fridolfsson HN. Interactions between nuclei and the cytoskeleton are mediated by SUN-KASH nuclear-envelope bridges. *Annu Rev Cell Dev Biol* 2010; 26:421-44; PMID:20507227; <http://dx.doi.org/10.1146/annurev-cellbio-100109-104037>
3. Gundersen GG, Worman HJ. Nuclear positioning. *Cell* 2013; 152:1376-89; PMID:23498944; <http://dx.doi.org/10.1016/j.cell.2013.02.031>
4. Razafsky D, Wirtz D, Hodzic D. Nuclear Envelope in Nuclear Positioning and Cell Migration. In: Schirmer EC, de las Heras JJ, eds. *Cancer Biology and the Nuclear Envelope*; Springer New York, 2014:471-90.
5. Mejat A, Misteli T. LINC complexes in health and disease. *Nucleus* 2010; 1:40-52; PMID:21327104; <http://dx.doi.org/10.4161/nucl.1.1.10530>
6. Stroud MJ, Banerjee I, Veevers J, Chen J. Linker of nucleoskeleton and cytoskeleton complex proteins in cardiac structure, function, and disease. *Circ Res* 2014; 114:538-48; PMID:24481844; <http://dx.doi.org/10.1161/CIRCRESAHA.114.301236>
7. Isermann P, Lammerding J. Nuclear mechanics and mechanotransduction in health and disease. *Curr Biol* 2013; 23:R1113-21; PMID:24355792; <http://dx.doi.org/10.1016/j.cub.2013.11.009>
8. Tamura K, Hara-Nishimura I. Involvement of the nuclear pore complex in morphology of the plant nucleus. *Nucleus* 2011; 2:168-72; PMID:21818409; <http://dx.doi.org/10.4161/nucl.2.3.16175>
9. Chytilova E, Macas J, Sliwinski E, Rafelski SM, Lambert GM, Galbraith DW. Nuclear dynamics in *Arabidopsis thaliana*. *Mol Biol Cell* 2000; 11:2733-41; PMID:10930466
10. Zhou X, Graumann K, Evans DE, Meier I. Novel plant SUN-KASH bridges are involved in RanGAP anchoring and nuclear shape determination. *J Cell Biol* 2012; 196:203-11; PMID:22270916; <http://dx.doi.org/10.1083/jcb.201108098>
11. Tamura K, Iwabuchi K, Fukao Y, Kondo M, Okamoto K, Ueda H, Nishimura M, Hara-Nishimura I. Myosin XI-1 links the nuclear membrane to the cytoskeleton to control nuclear movement and shape in *Arabidopsis*. *Curr Biol* 2013; 23:1776-81; PMID:23973298; <http://dx.doi.org/10.1016/j.cub.2013.07.035>
12. Oda Y, Fukuda H. Dynamics of *Arabidopsis* SUN proteins during mitosis and their involvement in nuclear shaping. *Plant J* 2011; 66:629-41; PMID:21294795
13. Zhao Q, Brkljacic J, Meier I. Two distinct interacting classes of nuclear envelope-associated coiled-coil proteins are required for the tissue-specific nuclear envelope targeting of *Arabidopsis* RanGAP. *Plant Cell* 2008; 20:1639-51; PMID:18591351; <http://dx.doi.org/10.1105/tpc.108.059220>
14. Houben F, Ramaekers FC, Snoeckx LH, Broers JL. Role of nuclear lamina-cytoskeleton interactions in the maintenance of cellular strength. *Biochim Biophys*

- Acta* 2007; 1773:675-86; PMID:17050008; <http://dx.doi.org/10.1016/j.bbamer.2006.09.018>
15. Ciska M, Moreno Diaz de la Espina S. The intriguing plant nuclear lamina. *Front Plant Sci* 2014; 5:166; PMID:24808902; <http://dx.doi.org/10.3389/fpls.2014.00166>
16. Masuda K, Xu ZJ, Takahashi S, Ito A, Ono M, Nomura K, Inoue M. Peripheral framework of carrot cell nucleus contains a novel protein predicted to exhibit a long alpha-helical domain. *Exp Cell Res* 1997; 232:173-81; PMID:9141634; <http://dx.doi.org/10.1006/excr.1997.3531>
17. Masuda K, Haruyama S, Fujino K. Assembly and disassembly of the peripheral architecture of the plant cell nucleus during mitosis. *Planta* 1999; 210:165-7; PMID:10592045; <http://dx.doi.org/10.1007/s004250050666>
18. Ciska M, Masuda K, Moreno Diaz de la Espina S. Lamin-like analogues in plants: the characterization of NMCP1 in *Allium cepa*. *J Exp Bot* 2013; 64:1553-64; PMID:23378381; <http://dx.doi.org/10.1093/jxb/ert020>
19. Sakamoto Y, Takagi S. LITTLE NUCLEI 1 and 4 regulate nuclear morphology in *Arabidopsis thaliana*. *Plant Cell Physiol* 2013; 54:622-33; PMID:23396599; <http://dx.doi.org/10.1093/pcp/pct031>
20. Dittmer TA, Stacey NJ, Sugimoto-Shirasu K, Richards EJ. LITTLE NUCLEI genes affecting nuclear morphology in *Arabidopsis thaliana*. *Plant Cell* 2007; 19:2793-803; PMID:17873096
21. Wang H, Dittmer TA, Richards EJ. *Arabidopsis* CROWDED NUCLEI (CRWN) proteins are required for nuclear size control and heterochromatin organization. *BMC Plant Biol* 2013; 13:200; PMID:24308514; <http://dx.doi.org/10.1186/1471-2229-13-200>
22. Graumann K. Evidence for LINC1-SUN associations at the plant nuclear periphery. *PLoS One* 2014; e93406; PMID: 24667841; <http://dx.doi.org/10.1371/journal.pone.0093406>
23. Zhou X, Meier I. Efficient plant male fertility depends on vegetative nuclear movement mediated by two families of plant outer nuclear membrane proteins. *Proc Natl Acad Sci USA* 2014; 111:11900-5; PMID:25074908
24. Avisar D, Abu-Abied M, Belasov E, Sador E, Hawes C, Sparkes IA. A comparative study of the involvement of 17 *Arabidopsis* myosin family members on the motility of Golgi and other organelles. *Plant Physiol* 2009; 150:700-9; PMID:19369591; <http://dx.doi.org/10.1104/pp.109.136853>
25. Graumann K, Runions J, Evans DE. Characterization of SUN-domain proteins at the higher plant nuclear envelope. *Plant J* 2010; 61:134-44; PMID:19807882; <http://dx.doi.org/10.1111/j.1365-313X.2009.04038.x>
26. Zhou X, Graumann K, Wirthmueller L, Jones JDG, Meier I. Identification of unique SUN-interacting nuclear envelope proteins with diverse functions in plants. *J Cell Bio* 2014; 205:677-92; PMID:24891605; <http://dx.doi.org/10.1083/jcb.201401138>

Disclosure of Potential Conflicts of Interest

No potential conflicts of interest were disclosed.

Funding

We thank the National Science Foundation for financial support (NSF-MCB 1243844).

Supplemental Material

Supplemental data for this article can be accessed on the publisher's website.

- PMID:24891605; <http://dx.doi.org/10.1083/jcb.201401138>
27. Goto C, Tamura K, Fukao Y, Shimada T, Hara-Nishimura I. The Novel Nuclear Envelope Protein KAKU4 Modulates Nuclear Morphology in *Arabidopsis*. *Plant Cell* 2014; 26:2143-55; PMID:24824484
28. Tamura K, Fukao Y, Iwamoto M, Haraguchi T, Hara-Nishimura I. Identification and characterization of nuclear pore complex components in *Arabidopsis thaliana*. *Plant Cell* 2010; 22:4084-97; PMID:21189294; <http://dx.doi.org/10.1105/tpc.110.079947>
29. Tamura K, Hara-Nishimura I. The molecular architecture of the plant nuclear pore complex. *J Exp Bot* 2013; 64:823-32; PMID:22987840; <http://dx.doi.org/10.1093/jxb/ers258>
30. Libotte T, Zaim H, Abraham S, Padmakumar VC, Schneider M, Lu W, Munck M, Hutchison C, Wehnert M, Fahrenkrog B, et al. Lamin A/C-dependent localization of Nesprin-2, a giant scaffold at the nuclear envelope. *Mol Biol Cell* 2005; 16:3411-24; PMID:15843432; <http://dx.doi.org/10.1091/mbc.E04-11-1009>
31. Haque F, Lloyd DJ, Smallwood DT, Dent CL, Shanahan CM, Fry AM, Trembath RC, Shackleton S. SUN1 interacts with nuclear lamin A and cytoplasmic nesprins to provide a physical connection between the nuclear lamina and the cytoskeleton. *Mol Cell Biol* 2006; 26:3738-51; PMID:16648470; <http://dx.doi.org/10.1128/MCB.26.10.3738-3751.2006>
32. Haque F, Mazzeo D, Patel JT, Smallwood DT, Ellis JA, Shanahan CM, Shackleton S. Mammalian SUN protein interaction networks at the inner nuclear membrane and their role in laminopathy disease processes. *J Biol Chem* 2010; 285:3487-98; PMID:19933576; <http://dx.doi.org/10.1074/jbc.M109.071910>
33. Kracklauer MP, Banks SML, Xie XH, Wu YN, Fischer JA. *Drosophila* klaroid encodes a SUN domain protein required for Klarisicht localization to the nuclear envelope and nuclear migration in the eye. *Fly* 2007; 1:75-85; PMID:18820457
34. Patterson K, Molofsky AB, Robinson C, Acosta S, Cater C, Fischer JA. The functions of Klarisicht and nuclear lamin in developmentally regulated nuclear migrations of photoreceptor cells in the *Drosophila* eye. *Mol Biol Cell* 2004; 15:600-10; PMID:14617811
35. Griffis AH, Groves NR, Zhou X, Meier I. Nuclei in motion: movement and positioning of plant nuclei in development, signaling, symbiosis, and disease. *Front Plant Sci* 2014; 5:129; PMID:24772115; <http://dx.doi.org/10.3389/fpls.2014.00129>
36. Takagi S, Islam MS, Iwabuchi K. Chapter four - Dynamic Behavior of Double-Membrane-Bounded Organelles in Plant Cells. In: Kwang WJ, ed. *Int Rev Cell Mol Biol*; Academic Press, 2011:181-222.
37. Xu XM, Meulia T, Meier I. Anchorage of plant RanGAP to the nuclear envelope involves novel nuclear-pore-associated proteins. *Curr Biol* 2007; 17:1157-63; PMID:17600715; <http://dx.doi.org/10.1016/j.cub.2007.05.076>

38. Karimi M, Inze D, Depicker A. GATEWAY™ vectors for *Agrobacterium* -mediated plant transformation. Trends Plant Sci 2002; 7:193-5; PMID:11992820
39. Nakagawa T, Kurose T, Hino T, Tanaka K, Kawamukai M, Niwa Y, Toyooka K, Matsuoka K, Jinbo T, Kimura T. Development of series of gateway binary vectors, pGWBs, for realizing efficient construction of fusion genes for plant transformation. J Biosci Bioeng 2007; 104:34-41; PMID:17697981; <http://dx.doi.org/10.1263/jbb.104.34>
40. Wise AA, Liu Z, Binns AN. Three methods for the introduction of foreign DNA into *Agrobacterium*. Methods Mol Biol 2006; 343:43-53; PMID:16988332; <http://dx.doi.org/10.1385/1-59745-130-4:43>
41. Clough SJ, Bent AF. Floral dip: a simplified method for *Agrobacterium* -mediated transformation of *Arabidopsis thaliana*. Plant J 1998; 16:735-43; PMID:10069079

Copyright of Nucleus (1949-1034) is the property of Landes Bioscience and its content may not be copied or emailed to multiple sites or posted to a listserv without the copyright holder's express written permission. However, users may print, download, or email articles for individual use.